Synthesis and Catalytic Properties of Heterobimetallic Complexes of the Tripod Ligand $HC(PPh_2)_3$. X-ray Molecular Structures of $[Rh(COD)\{HC(PPh_2)_3\}Au(PPh_3)](BF_4)_2$ and $[RhCu_2\{HC(PPh_2)_3\}_2(THF)_2(CH_3CN)_2](BF_4)_2(F)$

H. El-Amouri,† A. A. Bahsoun, J. Fischer, J. A. Osborn,* and M.-T. Youinou

Laboratoire de Chimie des Métaux de Transition et de Catalyse, UA au CNRS No. 424, Institut Le Bel, Université Louis Pasteur, 4 rue Blaise Pascal, 67000 Strasbourg, France

Received March 1, 1991

Treatment of $[M(COD)\{HC(PPh_2)_3\}]BF_4$ (M = Rh, Ir; **1a**, **1b**) with 1 equiv of the complex $[Au(PPh_3)(THF)]BF_4$ in THF/CH_2Cl_2 at room temperature afforded the binuclear species $[M(COD)\{HC(PPh_2)_3\}Au(PPh_3)](BF_4)_2$ (M = Rh, Ir; **2a**, **2b**). The molecular structure of **2a** showed both rhodium and gold bound to a single tripod ligand in a clamped arrangement with a rhodium to gold separation of 5.431 (1) Å. The reactions of molecular hydrogen and carbon monoxide with these complexes have been studied. When the mononuclear species $[Rh(COD)\{HC(PPh_2)_3\}]BF_4$ (**1a**) was treated with $[Cu(CH_3CN)_4]BF_4$ in acetonitrile, the heterobinuclear complex $[Rh(CH_3CN)_3Cu\{HC(PPh_2)_3\}](BF_4)_2$ (**6**) was obtained. **6** transforms in CH_2Cl_2/THF to give the trinuclear species $[RhCu_2\{HC(PPh_2)_3\}_2(THF)_2(CH_3CN)_2](BF_4)_2(F)$ (**7**) for which an X-ray molecular structure was also determined. In the structure the rhodium lies on a center of symmetry, the two copper(I) ions each being 5.353 (4) Å distant from rhodium. The tetracoordinate planar arrangement of four phosphorus atoms about the rhodium results from the coordination of two tripod ligands, each providing two donor sites, leaving one phosphorus atom on each tripod to bind each Cu(I), which possesses a trigonal-planar coordination geometry. The catalytic properties of these new complexes for the hydrogenation of olefins have been briefly compared in order to probe the effect of the presence of the coinage metal on such processes. $2a \cdot 2H_2O \cdot Et_2O$ crystallizes in the monoclinic space group $P2_1/n$ (No. 14), a = 20.704 (5) Å, b = 13.686 (3) Å, c = 23.573 (5) Å, β = 109.42 (2)°, and Z = 4. The structure was refined to R = 6.4 and R_w = 10.7%, using 6924 reflections. $7 \cdot 2C_6H_6$ crystallizes in the triclinic space group $P\bar{1}$ (No. 2), a = 13.544 (3) Å, b = 14.741 (3) Å, c = 13.156 (3) Å, α = 101.69 (2)°, β = 98.29 (2)°, γ = 62.76 (2)°, and Z = 1. The structure was refined to R = 10.1 and R_w = 13.6%, using 4437 reflections.

Introduction

The addition of a coinage metal (M = Cu, Ag, Au) to a platinum group metal (M′) often has a profound effect on catalytic activity in heterogeneous systems.[1] Numerous mixed-metal complexes containing a coinage metal and a platinum metal have been synthesized in recent years. In this work several molecular bimetallic complexes of Rh or Ir containing Au or Cu moieties have been studied in an attempt to investigate the effect of the proximity of the coinage metals on catalytic properties in a homogeneous system. The starting point for our studies involved the complexes $[M(COD)\{HC(PPh_2)_3\}]BF_4$ (M = Rh, Ir; COD = 1,5-cyclooctadiene; **1a,b**) where we have previously shown that only two phosphorus atoms of the $HC(PPh_3)_2$(tripod) are bound to M, the third donor atom remaining uncoordinated, thereby being potentially available for the coordination of a further metal species.[2] The analogous homobinuclear complex $[Rh_2(COD)S_2\{HC(PPh_2)_3\}]^{2+}$ had been synthesized in this manner and was found to be active in the catalytic hydrogenation of olefins.[3] Further, since we have found that **1a** can also serve as such a catalyst, the preparation and study of some corresponding heterobimetallic complexes containing coinage metals were carried out to probe the effect on this catalytic process.

Results and Discussion

Synthesis and Characterization of $[M(COD)\{HC(PPh_2)_3\}(Au(PPh_3)](BF_4)_2$ (M = Rh, Ir; 2a,b). The complexes $[M(COD)\{HC(PPh_2)_3\}Au(PPh_3)](BF_4)_2$ (M = Rh, Ir; **2a,b**) were prepared in high yield by addition of 1 equiv of $[Au(PPh_3)(THF)]BF_4$ to $[M(COD)\{HC(PPh_2)_3\}]BF_4$ according to the following reaction scheme:

$$[Au(PPh_3)Cl] + AgBF_4 \xrightarrow{THF} [Au(PPh_3)(THF)]BF_4 + AgCl$$

$$[Au(PPh_3)(THF)]BF_4 + [M(COD)\{HC(PPh_2)_3\}]BF_4 \xrightarrow{THF/CH_2Cl_2} \mathbf{2a,b}\ (M = Rh, Ir)$$

Complexes **2a,b** were characterized by standard methods, in particular NMR spectroscopy, as well as by an X-ray structural determination of **2a**. The ^{31}P NMR spectrum of **2a** (Figure 1) consists of two well-separated regions, which can be interpreted overall in terms of a ABM_2X spin system. Centered at −5.4 ppm is a pair of doublets, which are assigned to two equivalent phosphorus atoms (P_1,P_2 = M) of the tripod ligand, which chelate the Rh(I) atom (X). The large doublet coupling ^1J(Rh–P) = 136 Hz is further split by coupling (^2J = 9 Hz) to P_3 (A), being the phosphorus atom of the tripod ligand not coordinated to Rh(I). At low field, the spectrum has the appearance of a perturbed AB spectrum centered at 43 ppm. The lower half-field of this spectrum shows two lines of unequal intensity arising predominantly from P_4 (B) of the PPh_3 ligand bound to Au, where the P_4 nucleus is strongly coupled to P_3 (A) of the tripod ligand with $^2J(P_3–P_4)$ = 329 Hz. The upfield A part, largely resulting from the P_3 resonance, also appears as two lines of unequal intensity but now each splits into apparent triplets, arising

† Present address: Laboratoire de Chimie Organométallique, UA au CNRS No. 403, Ecole Nationale de Chimie de Paris, 11 rue Pierre et Marie Curie, 75005 Paris.

(1) (a) Clarke, J. K. A. *Chem. Rev.* **1975**, *75*, 291. (b) Balakrishnan, K.; Sachdev, A.; Schwank, J. *J. Catal.* **1990**, *121*, 441 and references herein.

(2) El-Amouri, H.; Bahsoun, A. A.; Osborn, J. A. *Polyhedron* **1988**, *7*, 2035.

(3) El-Amouri, H.; Bahsoun, A. A.; Fischer, J.; Osborn, J. A. *Angew. Chem., Int. Ed. Engl.* **1987**, *26*, 1169.

0276-7333/91/2310-3582$02.50/0 © 1991 American Chemical Society

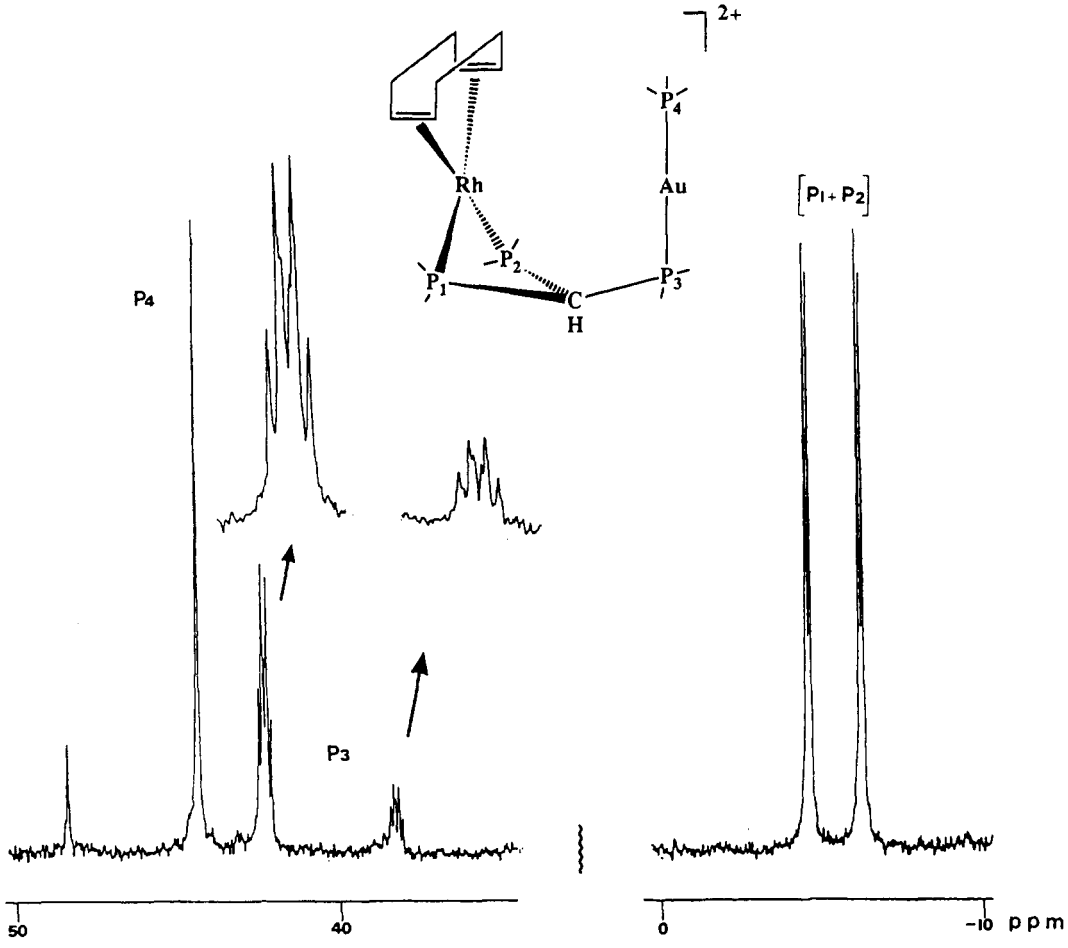

Figure 1. $^{31}P\{^1H\}$ NMR spectrum of **2a** in a $(CD_3)_2CO/(CH_3)_2CO$ solution.

from coupling of P_3 to P_1 and P_2 (9 Hz) as well as to Rh with $^3J(Rh-P_3)$ = 10 Hz.

The analogous Ir compound **2b** shows a similar ABM_2 ^{31}P NMR spectrum, the M_2 part now appearing as a doublet at −17.2 ppm, whereas the AB part of spectrum is now centered at 44.3 ppm with $^2J(P_3-P_4)$ = 328 Hz and $^2J(P_1-P_3) = {}^2J(P_2-P_3)$ = 6 Hz.

A bimetallic structure can be proposed for **2a** (and **2b**) as shown.

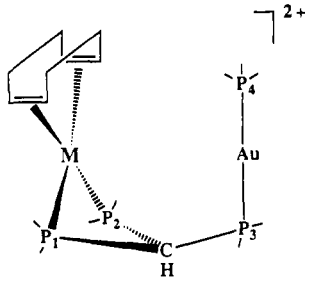

M=Rh, 2a; Ir, 2b

The NMR data do not allow us to determine whether a M–Au interaction exists or not in solution. We note that the coupling constant $^3J(Rh-P_3)$ increased from 3 Hz in the mononuclear species **1a**[2] to 10 Hz in the binuclear complex **2a**, which could be taken as possible evidence for the existence of a Rh–Au interaction but, given that no apparent coupling was observed in **2a** between P_4 and Rh, this is not convincing. Consequently suitable crystals of **2a** were grown for an X-ray structure determination.

The X-ray structure of **2a**·$2H_2O$·Et_2O, which is shown in Figure 2, consists of a $[Rh(COD)\{HC(PPh_2)_3\}Au(PPh_3)]^{2+}$ cation, two BF_4^- anions, and solvated molecules of water and ether. Table I lists positional parameters for the important atoms and in Table II selected bond distances and bond angles are collected. The rhodium(I) atom is in the expected square-planar arrangement surrounded by the two olefin groups of the cyclooctadiene

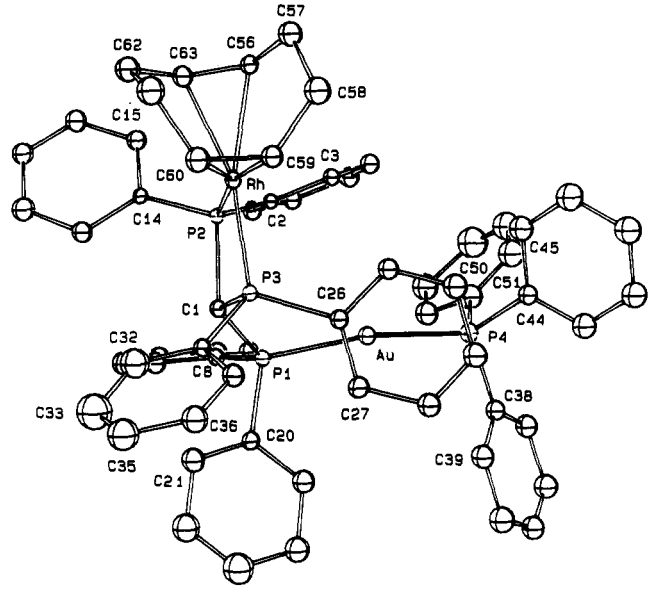

Figure 2. ORTEP plot of one molecule of **2a**·$2H_2O$·Et_2O showing the numbering scheme used (in a given ring, only the two first atoms are numbered for clarification of the figure). Ellipsoids are scaled to enclose 50% of the electronic density. Hydrogen atoms are omitted.

Scheme I

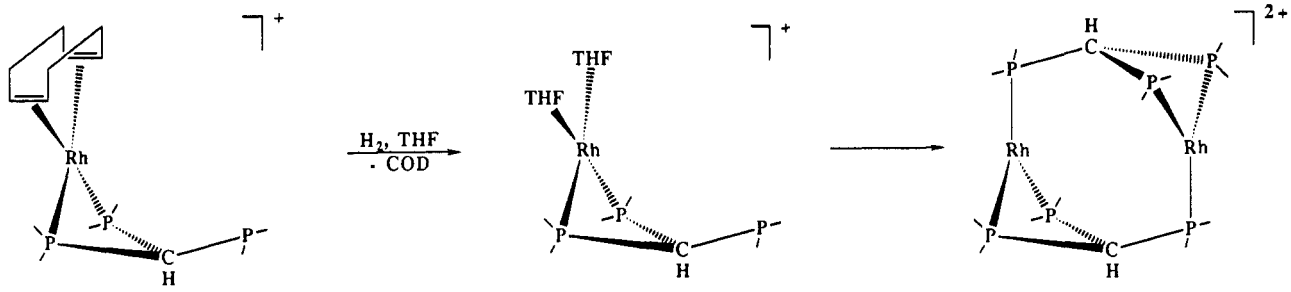

Table I. Table of Positional Parameters in $2a \cdot 2H_2O \cdot Et_2O$ for Selected Atoms and Their Esd's

atom	x	y	z	B, Å²
Au	-0.18573 (2)	-0.13071 (4)	0.15155 (2)	2.93 (1)
Rh	0.01051 (4)	0.12940 (6)	0.16294 (4)	2.24 (2)
P1	-0.0775 (2)	-0.1543 (2)	0.2204 (1)	2.34 (6)
P2	-0.0293 (1)	0.0698 (2)	0.2343 (1)	2.07 (6)
P3	0.0059 (1)	-0.0334 (2)	0.1503 (1)	2.11 (6)
C1	-0.0123 (6)	-0.0648 (8)	0.2211 (5)	2.4 (3)
P4	-0.2985 (2)	-0.1392 (3)	0.0896 (2)	3.54 (8)
C56	-0.0154 (6)	0.2906 (8)	0.1580 (6)	3.2 (3)
C57	-0.0175 (7)	0.328 (1)	0.0950 (6)	4.0 (3)
C58	-0.0104 (8)	0.249 (1)	0.0521 (7)	4.9 (4)
C59	0.0323 (6)	0.165 (1)	0.0783 (6)	3.3 (3)
C60	0.0939 (7)	0.167 (1)	0.1257 (7)	4.6 (3)
C61	0.1307 (7)	0.258 (1)	0.1537 (8)	5.5 (4)
C62	0.1125 (8)	0.293 (1)	0.2067 (8)	5.2 (4)
C63	0.0412 (7)	0.2795 (9)	0.2050 (6)	3.3 (3)

ligand and two phosphorus atoms of the tripod ligand. The third P atom of the tripod ligand is bonded to a $AuPPh_3$ group, forming a two-coordinate linear geometry about the gold atom. The Rh–Au distance of 5.431 (1) Å would thus preclude any significant interaction between the two metal centers in the solid state. We note that in a reported structure[4] for the complex $[RhAu(PNP)_2]^+$ where *two* clamplike tridentate ligands (PNP = 2-bis(diphenylphosphino)methylpyridine) bind Rh(I) and Au(I) in close proximity, a Rh–Au bond is formed with a distance between the metals of 2.85 Å.

Reactivity of $[M(COD)\{HC(PPh_2)_3\}]BF_4$ (1a,b) and $[M(COD)\{HC(PPh_2)_3\}Au(PPh_3)](BF_4)_2$ (2a,b) with H_2. When an orange $(CD_3)_2CO$ solution of the mononuclear complex $[Rh(COD)\{HC(PPh_2)_3\}]^+$ **1a** was treated with dihydrogen at room temperature, the ^1H NMR spectrum shows the appearance of a singlet at 1.5 ppm. This is attributable to cyclooctane formation by hydrogenation of the 1,5-cyclooctadiene ligand. No hydride resonances are detected. The solvated species $[Rh\{HC(PPh_2)_3\}((CD_3)_2CO)_2]^+$ may be formed analogous to other solvates such as $[Rh(dppe)(THF)_2]^+$ (dppe = bis(diphenylphosphino)ethane) that are also known to be obtained by this method.[5] However, after 4 h the ^{31}P NMR spectrum evolved with the disappearance of the above doublet resonance and the formation of two sets of peaks in a ratio 1:2, consisting of a doublet of multiplets centered at 37 ppm with $^1J(P–Rh) = 117$ Hz and $^2J(P–P) = 17$ Hz, along with a doublet of triplets centered at 6.5 ppm with $^1J(P–Rh) = 107$ Hz and $^2J(P–P) = 17$ Hz. We tentatively propose that a homobinuclear species $[Rh\{HC(PPh_2)_3\}]_2^{2+}$ is formed in which each Rh(I) center is bound to three phosphorus nuclei with the two tripod ligands oriented in a head–tail fashion (see Scheme I).

(4) McNair, R. J.; Nilsson, P. V.; Pignolet, L. H. *Inorg. Chem.* **1985**, *24*, 1935.
(5) (a) Schrock, R. R.; Osborn, J. A. *J. Am. Chem. Soc.* **1976**, *98*, 4450. (b) Halpern, J. H.; Riley, D. P.; Chan, A. S. C.; Pluth, J. J. *J. Am. Chem. Soc.* **1977**, *99*, 8055.

Table II. Selected Distances (Å) and Bond Angles (deg) for $2a \cdot 2H_2O \cdot Et_2O$[a]

dist, Å		bond angles, deg	
Au-P1	2.311 (2)	P1-Au-P4	167.87 (8)
Au-P4	2.308 (2)	P2-Rh-P3	74.34 (7)
Rh-P2	2.257 (2)	P2-Rh-C56	104.6 (2)
Rh-P3	2.246 (2)	P2-Rh-C59	166.8 (2)
Rh-C56	2.264 (8)	P2-Rh-C60	153.4 (3)
Rh-C59	2.240 (9)	P2-Rh-C63	96.9 (2)
Rh-C60	2.24 (1)	P2-Rh-C56	163.9 (2)
Rh-C63	2.277 (8)	P3-Rh-C59	96.3 (2)
		P3-Rh-C60	100.3 (3)
		P3-Rh-C63	161.1 (2)
		C56-Rh-C59	81.7 (3)
		C56-Rh-C60	87.5 (3)
		C56-Rh-C63	34.0 (3)
		C59-Rh-C60	36.1 (4)
		C59-Rh-C63	94.7 (3)
		C60-Rh-C63	79.9 (4)

[a] Estimated standard deviations are given in parentheses.

This compound would thus be formed by dimerization of $[Rh\{HC(PPh_2)_3\}\{(CD_3)_2CO\}_2]^+$. Attempts to characterize this complex further are under way, in particular to determine the presence or absence of a rhodium to rhodium interaction. The complex **2a** reacts also with H_2, slowly liberating cyclooctane. The ^{31}P NMR spectrum of the hydrogenated solution after 30 min shows the growth of a low-intensity doublet at 2.7 ppm with $J(Rh–P) = 117$ Hz and some weak peaks, somewhat obscured by the spectrum of **2a**, which later is seen to be an AB system centered at 44 ppm ($J(P_3–P_4) = 290$ Hz, $\delta(P_3)$ and $\delta(P_4)$ at 42.4 and 45.6 ppm). After several hours, the spectrum of **2a** has totally disappeared and the above spectrum is joined by that of a new species, which again shows an ABM_2X-type spectrum ($\delta_M = 10.9$ ppm, $J(Rh–P) = 174$ Hz; $J(P_3–P_4) = 310$ Hz, $\delta(P_3)$ and $\delta(P_4)$ at 37 and 45 ppm). The reaction of **2a** with dihydrogen is considerably slower than with **1a**, which yields a longer induction period in hydrogenation experiments (vide infra). However, the NMR spectra, although showing complex behavior, indicates that the $AuPPh_3$ unit remains bound after hydrogenation and no doubt serves to impede the dimerization process found in **2a**.

The reaction of $[Ir(COD)\{HC(PPh_3)_2\}]BF_4$ (**1b**) in CD_2Cl_2 with dihydrogen occurs rapidly at room temperature with a color change from purple to light yellow, but NMR studies indicate that decomposition of the reaction mixture takes place quite rapidly. When the reaction is carried out and studied by NMR spectroscopy at 260 K, a dihydride compound is formed resulting from the oxidative addition of dihydrogen to the Ir(I) atom. The ^1H NMR spectrum exhibits two sets of resonances consistent with terminal hydrides, namely, a triplet at -10.8 ppm ($^2J(H_a–P_1) = {}^2J(H_a–P_2) = 15$ Hz) and a doublet centered at -11.35 ppm ($^2J(H_b–P_1) = 110$ Hz). The ^1H spectrum also shows, apart from signals indicative of coordinated

Scheme II

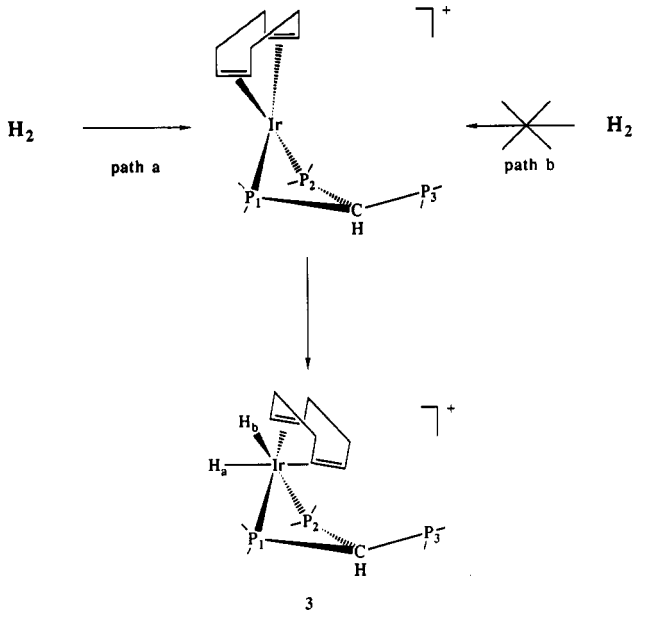

3

tripod ligand, the presence of an unsymmetrically coordinated COD ligand with four different vinyl resonances. From these data, we can propose that a mononuclear dihydrido complex $[IrH_2(COD)\{HC(PPh_2)_3\}]BF_4$ (**3**) (Scheme II) is formed with a structure similar to that proposed for the compound $[Ir(H_2(COD)(PPh_3)_2]BF_4$ prepared under similar experimental conditions.[6]

The ^{31}P NMR spectrum of **3** at 260 K in $(CD_3)_2CO/CH_2Cl_2$ solution exhibits three signals of equal intensity: a triplet at −20.0 ppm with $^2J(P_1-P_3) = 25$ Hz due to the uncoordinated P_3 of the tripod ligand and two quartets as −28 and −37 ppm with $^2J(P_1-P_3) = {}^2J(P_2-P_3) = 25$ Hz and $^2J(P_1-P_2) = 50$ Hz due to P_1 and P_2 nucleii, which chelate the Ir(III) center. Interestingly, the addition of dihydrogen to **1b** thus gives only one and not two products, since in principle this addition may proceed by two paths (see Scheme II). In path a, the hydrogen molecule adds to the Ir(I) center by approaching the square face distal to the uncoordinated phosphine ligand P_3, while in path b the hydrogen addition takes place via the face nearest to P_3. It appears that only one path occurs, probably path a, since steric effects created by the phenyl groups on P_3 would impede H_2 attack via path b.

Similarly, the bimetallic complex **2b** in CD_2Cl_2 reacts rapidly with dihydrogen at 298 K to give the bimetallic compound $[Ir(COD)H_2\{HC(PPh_2)_3\}Au(PPh_3)]^{2+}$ **4**. The ^1H NMR spectrum exhibits, besides typical signals indicative of the coordinated ligands $HC(PPh_2)_3$ and PPh_3, two sets of terminal hydride resonances, a triplet at −10.65 ppm (with $^2J(H_a-P_1) = {}^2J(H_a-P_2) = 15$ Hz) and a doublet centered at −11.20 ppm ($^2J(H_b-P_1) = 110$ Hz). The ^{31}P NMR spectrum of **4** recorded at room temperature in a $(CD_3)_2CO/(CH_3)_2CO$ solution exhibits an AB system centered at 43.5 ppm for (P_3, P_4) similar to that observed in complex **2b** with $^2J(P_3-P_4) = 328$ Hz. Two signals are observed for the P_1 and P_2 nuclei that chelate the Ir(III) center, each signal appearing as a doublet at −22.3 and −33.1 ppm, respectively with $^2J(P_1-P_2) = 57$ Hz. Therefore, a structure analogous to **3** is proposed for **4**.

It appears that there is no interaction between the iridium hydride ligands and Au, but this would not be surprising if the addition of H_2 to Ir(I) is on the square face distal from the Au(I) center. Certainly similar Ir/Au heterobinuclear complexes containing bridging hydrides are very stable[7] and their formation might be anticipated if addition were on the proximal face.

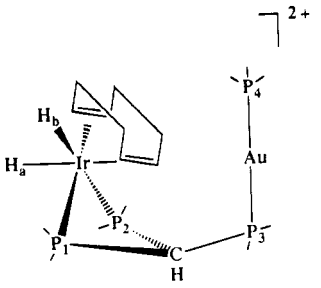

4

Hydrogenation of 1-Hexene Using the Catalyst Precursors 1a and 2a. $[Rh(COD)\{HC(PPh_2)_3\}]BF_4$ (**1a**) exhibits a modest catalytic activity in hydrogenation of 1-hexene under the normal experimental conditions (P = 1 atm of H_2, T = 25 °C), using a catalyst to substrate ratio of 1:150 with 5.4 mM of catalyst in 10 mL of 1,2-dichloroethane solution. An induction period of ca. 10–15 min is observed during which cyclooctane is liberated and the probable active species $[Rh\{HC(PPh_2)_3\}S_2]BF_4$ is generated. **1a** shows a turnover rate of 50 turnovers/h with an initial hydrogen uptake of 0.8 mL/min. There is an accompanying catalytic isomerization of the 1-hexene, the rate of which is slower (ca. three times) than that of the hydrogenation, producing *cis*- and *trans*-2-hexene (initial ratio 30:70). The internal olefins are not readily hydrogenated. After 4 h the catalyst became inactive and the ^{31}P NMR spectrum of the mixture obtained is similar to that of the dimeric complex $[Rh\{HC(PPh_2)_3\}]_2^{2+}$, suggesting that the deactivation of the catalyst is due to the formation of this dimer. Further, if the dimer is used separately, no activity for hydrogenation was found. Such irreversible aggregation of mononuclear catalysts to inactivate dimers or clusters is often the major cause of deactivation in homogeneous systems.

Under the same experimental conditions for the hydrogenation of 1-hexene, the rate of hydrogenation using $[Rh(COD)\{HC(PPh_2)_3\}Au(PPh_3)](BF_4)_2$ (**2a**) (ca. 0.4 mL/min) is slower than that observed with **1a** and occurs with a longer induction period (ca. 1 h). However, the lifetime of the catalyst is much longer than that of **1a** and all 1-hexene was consumed to give hexane (75%), *trans*-2-hexene (10%), and *cis*-2-hexene (15%). Further **2a** causes slightly less isomerization than that observed for **1a**. Both complexes **1a** and **2a** very slowly hydrogenated diphenylacetylene (100 equiv) in 1,2-dichloroethane to give *cis*-stilbene. Furthermore, in this case, concomitant catalyst deactivation led to only low overall conversion (ca. 20% for **1a**, 70% for **2a**).

In contrast to that observed with mononuclear **1a** (Rh) and heterobinuclear (Rh/Au) **2a** systems, **1b** and **2b** do not show any catalytic reactivity in hydrogenation of olefins under our standard conditions. The low catalytic activity usually found for iridium complexes such as **1b** and **2b** is generally thought to be related to the formation of strong, less reactive Ir–H bonds, e.g., as in $[IrH_2(PPh_3)_3Cl]$, an analogue of Wilkinson's catalyst. However,

(6) (a) Crabtree, R. H.; Felkin, H.; Morris, G. E. *J. Organomet. Chem.* **1977**, *141*, 205. (b) Crabtree, R. H.; Felkin, H.; Morris, G. E. *J. Chem. Soc., Chem. Commun.* **1976**, 716.

(7) For example: (a) Albinati, A.; Anklin, C.; Janser, P.; Lehner, H.; Matt, D.; Pregosin, P. S.; Venanzi, L. M. *Inorg. Chem.* **1989**, *28*, 1105. (b) Gomes Carneiro, T. M.; Matt, D.; Braunstein, P. *Coord. Chem. Rev.* **1989**, *96*, 49.

we note that catalysts[8] derived from $[Ir(COD)(Cy_3P)(py)]^+$ show very high hydrogenation activities in noncoordinated solvents, indicating that more subtle influences must be operative than are presently apparent.

Reactivity of $[Rh(COD)\{HC(PPh_2)_3\}Au(PPh_3)](BF_4)_2$ with CO. An orange CH_2Cl_2 solution of **2a** treated with carbon monoxide at 25 °C turned yellow rapidly, from which the bright yellow compound $[Rh(CO)_2\{HC(PPh_2)_3\}Au(PPh_3)](BF_4)_2$ (**5**) could be isolated. As a result of the lability of the CO ligands, **5** was rapidly precipitated, collected, and dried under a flow of CO. Two sharp carbonyl bands in the IR spectrum of **5** (CH_2Cl_2 solution) are observed at rather high frequencies for carbonyl groups trans to phosphorus atoms (2095 and 2060 cm^{-1}). The $^{31}P\{^1H\}$ NMR spectrum exhibits an AB system centered at 41.5 ppm, assigned to P_3 and P_4 with $^2J_{trans}(P_3-P_4)$ = 306 Hz, while a doublet of doublets at −8.0 ppm arises from the two phosphorus atoms of the ligand chelating the Rh(I) center with $^1J(Rh-P_1)$ = 107 Hz and $^2J(P_1-P_3)$ = 15 Hz. A structure analogous to that proposed for **2a** with two carbonyl ligands replacing the 1,5-cyclooctadiene is consistent with these data.

Synthesis and Characterization of the Heterobinuclear $[RhCu(CH_3CN)_3\{HC(PPh_2)_3\}](BF_4)_2$ (6) and $[RhCu_2\{HC(PPh_2)_3\}_2(THF)_2(CH_3CN)_2](BF_4)_2(F)$ (7). Upon treatment of $[Rh(COD)\{HC(PPh_2)_3\}]BF_4$ (**1a**) with 1 equiv of $[Cu(CH_3CN)_4]BF_4$ in acetonitrile solution, the color changes from orange to yellow and complex **6**, $[RhCu(CH_3CN)_3\{CH(PPh_2)_3\}](BF_4)_2$, is obtained in good yield by precipitation with ether.

$$[Cu(CH_3CN)_4]BF_4 + [Rh(COD)\{HC(PPh_2)_3\}]BF_4 \xrightarrow[CH_3CN]{-COD} [RhCu(CH_3CN)_3\{HC(PPh_2)_3\}](BF_4)_2$$

The infrared spectrum of $[RhCu(CH_3CN)_3\{HC(PPh_2)_3\}](BF_4)_2$ (**6**) in Nujol shows a strong absorption at 1050 cm^{-1}, corresponding to the presence of BF_4^- and weak bands at 2290 and 2305 cm^{-1} due to the symmetric and antisymmetric modes of C≡N of the coordinated acetonitrile ligands. Integration of the ^1H NMR spectrum of complex **6** shows the presence of one tripod ligand and three coordinated acetonitrile molecules in two different environments at 2.2 ppm (s, 3 H) and 1.96 ppm (s, 6 H), respectively. The ^{31}P NMR spectrum of **6** in $CD_3CN/(CH_3)_2CO$ exhibits two sets of signals, a doublet of doublets centered at 3.3 ppm assigned to P_1 and P_2 nuclei chelating the Rh(I) center with J(P–Rh) = 152 Hz, $J(P_1-P_3)$ = 14 Hz, and a broad triplet centered at −17.5 ppm resulting from the third phosphorus nucleus P_3 of the tripod ligand, which is bound to the Cu(I) atom. The structure of **6** is thus of the type shown for **2a**, with two CH_3CN ligands binding to Rh, the third CH_3CN completing a linear coordination about Cu(I). However, when the ^{31}P NMR spectrum of **6** was recorded in a CD_2Cl_2/CH_2Cl_2 mixture, the multiplets were in the same intensity ratio (2 P:1 P) but the doublet of doublets is now shifted to 12 ppm (J(P–Rh) = 145 Hz, $J(P_1-P_3)$ = 27 Hz), while the triplet is found at 5 ppm. In addition, a new set of doublet of doublets centered at −1 ppm begins to appear. In the absence of CH_3CN, **6** is not stable in CH_2Cl_2 solution and decomposes slowly to give this further species **7** (vide infra).

The spectroscopic results obtained do not allow us to eliminate the possibility of the presence of a Rh to Cu interaction for complex **6** but, given the structures found for **2a** (and **7**), an open form would appear most likely.

(8) Crabtree, R. H. *Acc. Chem. Res.* **1979**, *12*, 331.

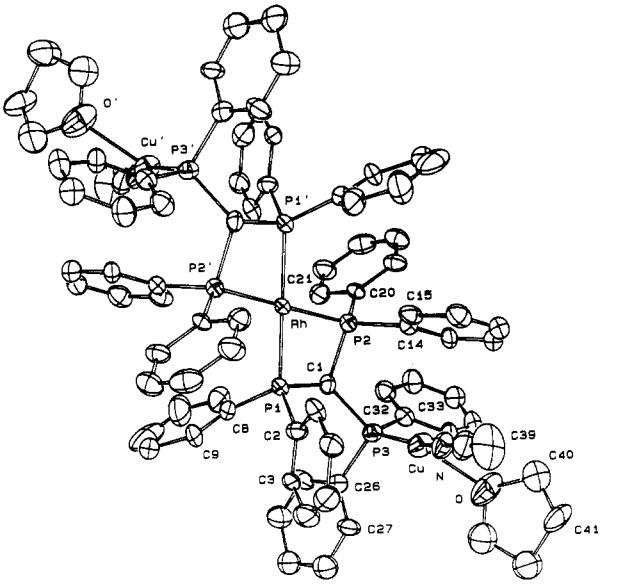

Figure 3. ORTEP plot of one molecule of $7\cdot 2C_6H_6$ showing the numbering scheme used (in a given ring, only the two first atoms are numbered for clarification of the figure). Ellipsoids are scaled to enclose 50% of the electronic density. Hydrogen atoms are omitted.

Table III. Table of Positional Parameters in $7\cdot 2C_6H_6$ for Selected Atoms and Their Esd's

atom	x	y	z	B, Å^2
Rh	0.500	0.500	0.500	2.68 (3)
Cu	0.1434 (1)	0.6338 (1)	0.2338 (1)	5.05 (5)
P1	0.4775 (2)	0.4679 (2)	0.3243 (2)	3.17 (7)
P2	0.3400 (2)	0.4823 (2)	0.4660 (2)	3.10 (7)
P3	0.2431 (2)	0.4681 (2)	0.2270 (2)	3.38 (7)
C1	0.3645 (8)	0.4306 (8)	0.3241 (9)	3.4 (3)
N	0.1105 (8)	0.7731 (7)	0.2607 (9)	4.5 (3)

Compound **7** was obtained accidentally, but later reproducibly, when recrystallization of complex **6** was attempted from $CH_2Cl_2/THF/C_6H_6$. After several hours a black precipitate (tentatively identified as Rh metal) was removed by filtration and benzene added to the filtrate. Yellow-orange crystals formed over the next few days, which were suitable for an X-ray diffraction analysis (vide infra). The IR of **7** (Nujol mull) shows the presence of BF_4^- at 1050 cm^{-1} and a weak band at 2290 cm^{-1} assigned as a C≡N vibration of coordinated CH_3CN. The ^1H NMR recorded in CD_3CN shows, by integration, the presence of CH_3CN (at 1.96 ppm) as well as two THF molecules. The ^{31}P NMR spectrum of **7** (CD_2Cl_2/CH_2Cl_2) exhibits a doublet centered at −1 ppm with J(P–Rh) = 115 Hz (2 P) and a broad triplet centered at 5.5 ppm (1 P) attributed to P_3 of the tripod ligand bound to the Cu center.

An X-ray structure served to detail the nature of the coordination about both metal ions in $[RhCu_2\{HC(PPh_2)_3\}_2(THF)_2(CH_3CN)_2](BF_4)_2(F)\cdot 2C_6H_6$. The unit cell contains one molecule of **7** as a tricationic species $[RuCu_2\{HC(PPh_2)_3\}_2(THF)_2(CH_3CN)_2]^{3+}$ with two molecules of BF_4^- and one fluoride atom (formed evidently by hydrolysis) as counteranions and two solvated benzene molecules. An ORTEP plot of the cation with the labeling scheme is shown in Figure 3. Selected positional parameters and intramolecular bond lengths and angles are respectively presented in Tables III and IV.

The rhodium atom of the complex cation **7** lies on an inversion center, the two Cu(I) and the Rh(I) ions are therefore in a linear arrangement with each (Rh, Cu) couple being bridged by a tripod ligand. The Rh–Cu separation of 5.353 (4) Å excludes any direct metal–metal

Table IV. Selected Distances (Å) and Bond Angles (deg) for 7·2C$_6$H$_6$[a]

dist, Å		bond angles, deg	
Rh-P1	2.269 (3)	P1-Rh-P2	74.0 (1)
Rh-P2	2.270 (3)	P1-Rh-P'2	106.0 (1)
Cu-P3	2.173 (3)	P3-Cu-N	157.9 (3)
Cu-N	1.86 (1)	P3-Cu-O	113.9 (3)
Cu-O	2.27 (1)	N-Cu-O	87.9 (4)

[a] Estimated standard deviations are given in parentheses.

interaction. The square-planar arrangement about the Rh ion is formed by four phosphorus atoms of the two tripod ligands. Due to the presence of the inversion center, the coordination geometry around each Cu atom is identical, being surrounded by one phosphorus donor of a tripod ligand and one molecule each of CH_3CN and THF. The four nuclei P_3, Cu, O(44), and N are coplanar within experimental error and form a trigonal-planar coordination geometry about each Cu. Complex **7** represents the first example in which two tripod ligands coordinate three metal centers in a linear fashion, similar to those known for the phosphine ligands of the type dmpa [[bis(diphenylphosphinomethyl)phenyl]arsine].[9] This is in contrast to the previously observed mode of coordination where the tripod ligand stabilizes three metal centers in a triangular form[10] or a triangular face of a cluster species.[11]

Complexes **6** and **7** failed to show any catalytic activity toward the hydrogenation of olefins under the normal conditions. In **6** this inactivity probably arises because of the presence of CH_3CN as ligand, which is not sufficiently labile to allow olefin to coordinate to Rh, and not because of the presence of Cu in the complex.

Conclusion

In summation, although the mechanism of the hydrogenation is not known for these systems, the presence of the coinage metal does not qualitatively change the catalytic properties. However, the increase in the steric factors caused by the presence of the additional metal and its ligands has the unfavorable effect of increasing the induction period and slowing the rate of catalysis but favorably increasing the stability of the catalyst. This latter stability arises no doubt by impeding the formation of inactive dimeric species. The fact that these systems do not show any effect of cooperative interaction between the metals may result from the flexibility of the tripod ligand, which fails to create sufficiently strong metal to metal interactions. However, we note that strong metal–metal bonds are found in certain cases, such as in Rh–Fe[12] and Rh–Rh[3] systems. More appropriately designed bimetallic systems will be necessary to probe the possible existence of such cooperative effects.

Experimental Section

All experiments were carried out under an atmosphere of prepurified nitrogen or argon, using Schlenk techniques, or performed in a Vacuum Atmospheres Corp. glovebox. Solvents were distilled from sodium benzophenone ketyl (hydrocarbon, Et_2O, and THF) or from CaH_2 (dichloromethane) under nitrogen. $Au(PPh_3)Cl$ (Strem Chemicals) and $AgBF_4$ (Fluka) were used without further purification. $[M(COD)\{HC(PPh_2)_3\}]BF_4$ (M = Rh, Ir) and $[Cu(CH_3CN)_4]BF_4$ were prepared according to literature methods.[2,13]

Infrared spectra were recorded on a Perkin-Elmer 597 spectrometer (Nujol mulls, reported in cm^{-1}). NMR spectra were recorded on a Bruker SY 200 (^1H, ^{31}P). Chemical shifts δ are referenced to $(CH_3)_4Si$ (^1H) or H_3PO_4 (^{31}P) in organic solvents, and couplings constants are reported in hertz. Elemental analyses were performed by the CNRS Microanalytical Laboratory at Lyon or at Strasbourg, France. Compounds often contained somewhat varying quantities (ca. 0.25–0.5 equiv measured by ^1H NMR) of CH_2Cl_2.

$[M(COD)\{HC(PPh_2)_3\}Au(PPh_3)](BF_4)_2$ (M = Rh, Ir; 2a,b).

2a. $Au(PPh_3)Cl$ (0.165 g, 0.34 mmol) dissolved in THF (5 mL) was treated with $AgBF_4$ (0.070 g, 0.36 mmol) and the resulting precipitate (AgCl) was filtered off. The colorless filtrate was added dropwise to a well-stirred solution of $[Rh(COD)\{HC(PPh_2)_3\}]BF_4$ (0.280 g, 0.34 mmol) in 20 mL of CH_2Cl_2 over 30 min. The resulting yellow-orange solution was concentrated under vacuum. Addition of excess Et_2O precipitated a microcrystalline deep yellow product, which was collected by filtration and dried under vacuum. The complex **2a** was recrystallized from CH_2Cl_2/Et_2O (yield 0.26 g, 80%). Anal. Calcd for $C_{63}H_{56}B_2F_8P_4RhAu\cdot{}^1/_4CH_2Cl_2$: C, 52.97; H, 4.08; P, 8.65. Found: C, 52.51, H, 4.24; P, 8.79. ^1H NMR (CD_2Cl_2) δ 7.9–6.7 (46 H, m, C_6H_5 and $HC(PPh_2)_3$), 5.3 (2 H, m, $=CH(COD)$), 4.5 (2 H, m, $=CH(COD)$), 2.7–1.5 (8 H, m, CH_2(COD)). $^{31}P\{^1H\}$NMR ($(CD_3)_2CO/(CH_3)_2CO$) δ 44.3 (P_4, PPh_3, $^2J(P_4-P_3)$ = 329 Hz), 42.7 (P_3, ($HC(P_3Ph_2)$, $^2J(P_3-P_4)$ = 329 Hz, $^2J(P_3-P_1)$ = 9 Hz, $^3J(P_3-Rh)$ = 10 Hz), -5.41 (dd, 2 P, (Ph_2P_1)-$HC(P_2Ph_2)$, $^1J(P_1-Rh)$ = 136 Hz, $^2J(P_1-P_3)$ = 9 Hz).

2b. The complex **2b** was obtained as described above, for **2a**, employing 0.25 mmol (0.237 g) of $Au(PPh_3)Cl$, 0.256 mmol (0.056 g) of $AgBF_4$, and 0.25 mmol (0.239 g) of $[Ir(COD)\{HC(PPh_2)_3\}]BF_4$. The purple microcrystalline complex **2b** was recrystallized from CH_2Cl_2/Et_2O (yield 0.225 g, 60%). Anal. Calcd for $C_{63}H_{58}B_2F_8P_4IrAu\cdot{}^1/_4CH_2Cl_2$: C, 49.86; H, 3.84; P, 8.15. Found: C, 48.46; H, 3.84; P, 8.11. ^1H NMR (CD_2Cl_2) δ 8.0–6.6 (46 H, m, C_6H_5 and $HC(PPh_2)_3$), 5.1–4.5 (4 H, m, $=CH(COD)$), 2.7–1.5 (8 H, d, $CH_2(COD)$). $^{31}P\{^1H\}$NMR ($(CD_3)_2CO$) δ 45.4 (1 P, d, P_4Ph_3, $^2J(P_4-P_3)$ = 328 Hz), 43.2 (1 P, dt, $HC(P_3Ph_2)$, $^2J(P_3-P_4)$ = 328 Hz, $^2J(P_1-P_3)$ = 6 Hz), -17.2 (2 P, d, $(Ph_2P_1)HC(P_2Ph_2)$, $^2J(P_1-P_3)$ = 6 Hz).

$[IrH_2(COD)\{HC(PPh_2)_3\}]BF_4$ (3). Molecular hydrogen was bubbled for 5 min into an NMR tube containing 10 mg (0.01 mmol) of $[Ir(COD)\{HC(PPh_2)_3\}]BF_4$ (**1b**) in a 2-mL mixture of $(CD_3)_2CO/CH_2Cl_2$ at T = 260 K. During this time the initial purple solution changes to light yellow; the $^{31}P\{^1H\}$NMR spectra were then recorded at the above temperature. ^1H NMR (CD_2Cl_2) δ 8.0–7.0 (30 H, m, C_6H_5), 5.0 (1 H, m, $CH(COD)$), 4.3 (1 H, m, $CH(COD)$), 4.1 (1 H, m, $CH(COD)$), 3.7 (1 H, m, $CH(COD)$), 2.4 (4 H, m, $CH_2(COD)$), 1.9 (4 H, m, $CH_2(COD)$), -10.8 (1 H, t, Ir-*H*, $^2J(P-H_{cis})$ = 15 Hz), -11.35 (1 H, d, Ir-*H*, $^2J(P-H_{trans})$ = 110 Hz). $^{31}P\{^1H\}$ NMR δ -20.0 (1 P, t, $HC(P_3Ph_2)$, $^2J(P_1-P_2)$ = 50 Hz, $^2J(P_2-P_3)$ = $^2J(P_1-P_3)$ = 25 Hz), -28.0 (1 P, q, $HC(P_2Ph_2)$), -37.0 (1 P, q, $HC(P_1Ph_2)$). The compound is unstable at room temperature and a satisfactory microanalysis was not obtained.

$[Ir(COD)H_2\{HC(PPh_2)_3\}Au(PPh_3)](BF_4)_2$ (4). Complex **4** was prepared in situ when molecular hydrogen was bubbled into a solution of **2b** in 2 mL of $(CD_3)_2CO/CH_2Cl_2$ (1:3) for few seconds, during which the color turned from purple to light yellow. ^1H NMR (CD_2Cl_2) δ -10.65 (1 H, t, Ir-*H*, $^2J(P_1-H_{cis})$ = 15 Hz), -11.25 (1 H, d, Ir-*H*), $^2J(P_1-H_{trans})$ = 110 Hz). $^{31}P\{^1H\}$ NMR (200 K, $(CD_3)_2CO$) δ (AB) 45.0 (1 P, P_4Ph_3), 42.2, (1 P, $HC(P_3Ph_2)$, $^2J(P_4-P_3)$ = 520 Hz), -22.3 (1 P, d, $HC(P_1Ph_2)$, $^2J(P_1-P_2)$ = 42.3 Hz), -33.6 (1 P, d, $HC(P_2Ph_2)$, $^2J(P_1-P_2)$ = -42.5 Hz). The compound is unstable at room temperature and a satisfactory microanalysis was not obtained.

$[Rh(CO)_2\{HC(PPh_2)_3\}Au(PPh_3)](BF_4)_2$ (5). CO was bubbled into an orange solution of **2a** (0.35 mmol, ca. 0.050 g) in CH_2Cl_2 (ca. 10 mL) for 10 min during which the color turned to yellow. Addition of cold Et_2O solution saturated with CO precipitates a bright yellow microcrystalline product **3**, which was recrystallized from CH_2Cl_2/Et_2O (yield 0.038 g, 80%). Anal. Calcd for

(9) Balch, A. L., Catalano, V. J.; Noll, B. C.; Olmstead, M. M. *J. Am. Chem. Soc.* **1990**, *112*, 7558 and references therein.
(10) Osborn, J. A.; Stanley, G. G. *Angew. Chem., Int. Ed. Engl.* **1980**, *19*, 1026.
(11) Bahsoun, A. A.; Osborn, J. A.; Voelker, C.; Bonnet, J. J.; Lavigne, G. *Organometallics* **1982**, *1*, 1114.
(12) Bahsoun, A. A.; Osborn, J. A.; Bird, P. H.; Nucciarone, D.; Peters, A. V. *Chem. Commun.* **1984**, 72.
(13) Shriver, D. F. *Inorganic Syntheses*; Wiley: New York, 1979; Collect. Vol. XIX; p 90.

Table V. X-ray Experimental Parameters

	2a·2H$_2$O·Et$_2$O	7·2C$_6$H$_6$
formula	$C_{67}H_{72}O_3P_4B_2F_8RhAu$	$C_{98}H_{96}N_2O_2P_6B_2F_9RhCu_2$
molec wt	1522.70	1942.31
color	orange yellow	yellow
cryst syst	monoclinic	triclinic
a, Å	20.704 (5)	13.544 (3)
b, Å	13.686 (3)	14.741 (3)
c, Å	23.573 (5)	13.156 (3)
α, deg		101.69 (2)
β, deg	109.42 (2)	98.29 (2)
γ, deg		62.76 (2)
V, Å^3	4667.3	2282.9
Z	4	1
D_{calc}, g cm^{-3}	1.605	1.413
space group	$P2_1/n$ (No. 14)	$P\bar{1}$ (No. 2)
radiation	Mo Kα (graphite monochromated)	
wavelength, Å	0.71073	
μ, cm^{-1}	27.5	8.08
cryst size, mm	0.22 × 0.12 × 0.11	0.24 × 0.20 × 0.10
temp	−100 °C	
diffractometer	Philips PW1100/16	
mode	$\theta/2\theta$ flying step scan	
scan speed, deg s^{-1}	0.024	
scan width, deg	1.00 + 0.343 tan θ	
step width, deg	0.05	
θ limits, deg	3/50	3/52
octants	$\pm h+k+l$	$\pm h\pm k+l$
no. of data collected	10547	7724
no. of data with $I > 3\sigma(I)$	6924	4437
abs, min/max	0.48/1.31	0.54/1.17
$R(F)$	0.064	0.101
$R_w(F)$	0.107	0.136
p	0.08	0.08
GOF	2.38	2.69

$C_{57}H_{46}P_4B_2F_8O_2RhAu$: C, 50.29; H, 3.38. With $^1/_4CH_2Cl_2$: C, 49.75, H, 3.40. Found: C, 49.33; H, 3.46. IR (CH_2Cl_2) ν(CO) 2095 (vs), 2060 (s) cm^{-1}. ^{1}H NMR (CD_2Cl_2) δ 8.0–6.8 (46 H, m, C_6H_5 and $HC(PPh_2)_3$). $^{31}P\{^1H\}$ NMR (254 K, $(CD_3)_2CO$) δ 46.4 (1 P, d, P_4Ph_3, $^2J(P_4–P_3)$ = 306 Hz), 36.7 (1 P, dt, $HC(P_3Ph_2)$, $^2J(P_3–P_4)$ = 306 Hz, $^2J(P_3–P_1)$ = 15 Hz), −8.0 (2 P, dd, $(Ph_2P_1)HC(P_2Ph_2)$, $^1J(P_1–Rh)$ = 107 Hz, $^2J(P_1–P_3)$ = 15 Hz).

[RhCu(CH$_3$CN)$_3${HC(PPh$_2$)$_3$}](BF$_4$)$_2$ (6). A solution of $[Cu(CH_3CN)_4]BF_4$ (0.25 mmol, 0.079 g) in acetonitrile (ca. 10 mL) was added at room temperature in a dropwise fashion to a vigourously stirred solution of [Rh(COD){HC(PPh$_2$)$_3$}]BF$_4$ (0.25 mmol, 0.216 g) in CH_2Cl_2 (ca. 10 mL) for 30 min. The yellow mother liquor solution was then concentrated and slow addition of Et_2O yielded a microcrystalline yellow product, which was collected, washed with C_6H_6 and Et_2O, and then dried under vacuum (yield 0.230 g, 90%). Anal. Calcd for $C_{43}H_{40}N_3P_3B_2F_8RhCu\cdot{}^1/_2CH_2Cl_2$: C, 48.61 H, 3.82; N, 3.91; P, 8.66. Found: C, 48.34; H, 4.00; N, 3.46; P, 8.47. ^{1}H NMR (CD_3CN) δ 7.9–7.0 (30 H, m, C_6H_5), 5.9 (1 H, m, $HC(PPh_2)_3$), 2.2 (3 H, s, CH_3CN), 1.96 (6 H, s, CH_3CN). $^{31}P\{^1H\}$ NMR ($(CD_3)_2CO/CH_3CN$) δ −3.3 (2 P, dd, $(Ph_2P_1)HC(P_2Ph_2)$, $^1J(Rh–P_1)$ = 152 Hz, $^2J(P_1–P_3)$ = 14 Hz), −17.5 (1 P, m (br), $HC(P_3Ph_2)$).

[RhCu$_2${HC(PPh$_2$)$_3$}$_2$(THF)$_2$(CH$_3$CN)$_2$](BF$_4$)$_2$(F) (7). A yellow solution made from 0.15 g of **6** dissolved into ca. 15 mL of CH_2Cl_2/THF (2:1 ratio) was stirred for several hours. The blackish precipitate that formed was removed by filtration and then an equal volume of C_6H_6 was added carefully to the filtrate. The mixture, left standing for several days, yielded crystals of 7·2C$_6$H$_6$, which were suitable to be used for the X-ray diffraction study. ^{1}H NMR (CD_3CN) δ 7.3–6.7 (60 H, m (br), C_6H_5), 6.0 (2 H, m, $HC(PPh_2)_3$), 3.5 (8 H, m, $(CH_2CH_2)_2O$), 1.96 (6 H, s, CH_3CN), 1.7 (8 H, m, $(CH_2CH_2)_2O$). $^{31}P\{^1H\}$ NMR (CD_2Cl_2) δ 5.4 (1 P, t (br)), −0.7 (2 P, d, ^1J(P–Rh) = 115 Hz).

X-ray Structure Determination. Single crystals of **2a** and **7** were obtained respectively by recrystallization from CH_2Cl_2/Et_2O and CH_2Cl_2/THF/C_6H_6 at room temperature. Crystals of both compounds were only marginally suitable for X-ray analysis. Systematic searches in reciprocal spaces at −100 °C using a Philips PW1100/16 automatic diffractometer showed that crystals of **2a**·2H$_2$O·Et$_2$O and 7·2C$_6$H$_6$ belong respectively to the monoclinic and triclinic systems.

Quantitative data were obtained at −100 °C, achieved by using a local-built gas flow device. All experimental parameters used are given in Table V. The resulting data sets were transferred to a VAX computer, and for all subsequent calculations the Enraf-Nonius SDP/VAX package[14] was used with the exception of a local data reduction program.

Three standard reflections measured every hour during the entire data collection period showed no significant trend.

The raw step-scan data were converted to intensities by using the Lehmann–Larsen method[15] and then corrected for Lorentz and polarization factors.

The structures were solved by using the heavy-atom method. After refinement of the heavy atoms, difference-Fourier maps revealed maxima of residual electronic density close to the positions expected for hydrogen atoms; they were introduced in structure factor calculations at their calculated coordinates (C–H = 0.95 Å) and isotropic temperature factors such as $B(H) = 1.3B_{eqv}(C)$ Å^2, but were not refined. For **2a**, the water hydrogen atoms were not introduced. At this stage empirical absorption corrections were applied by using the method of Walker and Stuart[16] since face indexation was not possible under the cold gas stream. Full least-squares refinements were carried out to convergence. Final difference maps revealed no significant maxima. The scattering factor coefficients[17a] and anomalous dispersion coefficients[17b] were taken from standard sources.

Hydrogenation of 1-Hexene with the Catalyst Precursors 1a and 2a. The hydrogenation experiments were carried out on a vacuum line apparatus similar to that previously reported,[18] using a catalyst to substrate ratio of 1:150. The catalyst precursors (0.054 mM) **1a** or **2a** dissolved in 10 mL of 1,2-dichloroethane solution were injected into a double-jacket flask. Freshly purified 1-hexene, 1 mL, was introduced to a flask attached to the double-jacket flask and the system was degassed thoroughly via three freeze–pump–thaw cycles. After the solution was warmed to room temperature, hydrogen was admitted (1 atm) and the volume of the hydrogen was measured on a graduated burrette. Then the olefin was transferred to the catalyst solution under constant stirring. Samples were periodically removed with a microsyringe and analyzed by gas chromatography. Identification of the peaks in the GC trace was carried out by comparison with authentic materials (Aldrich). Experiments were repeated three times to assure the reproducibility of the results.

Acknowledgment. We thank P. Maltèse for technical assistance in the NMR measurements and the C.N.R.S. for financial support.

Registry No. 1a, 123454-16-0; **1b**, 123454-18-2; **2a**, 135944-57-9; **2a**·2H$_2$O·Et$_2$O, 135944-68-2; **2b**, 135944-59-1; **3**, 135944-61-5; **4**, 135972-40-6; **5**, 135944-63-7; **6**, 135944-65-9; **7**, 135944-67-1; **7**·2C$_6$H$_6$, 135972-41-7; Au(PPh$_3$)Cl, 14243-64-2; $[Cu(CH_3CN)_4]BF_4$, 15418-29-8; 1-hexene, 592-41-6.

Supplementary Material Available: Tables S1 and S7, positional and thermal equivalent parameters for all non-hydrogen atoms, Tables S2 and S8, temperature factors for anisotropic atoms, Tables S3 and S9, hydrogen atom positional parameters, Tables S4 and S10, complete set of bond distances, and Tables S5 and S11, complete set of bond angles, for **2a** and **7**, respectively (29 pages); Tables S6 and S12, observed and calculated structure factor amplitudes for all observed reflections (44 pages). Ordering information is given on any current masthead page.

(14) Frenz, B. A. The Enraf-Nonius CAD4-SDP. In *Computing in Crystallography*; Schenk, H., Olthof-Hazekamp, R., Van Koningveld, H., Bassi, G. C., Eds.; University Press: Delft, Netherlands, 1978; p 64–71.
(15) Lehmann, M. S.; Larsen, F. K. *Acta Crystallogr.* **1974**, *A30*, 580.
(16) Walker, N.; Stuart, D. *Acta Crystallogr., Sect. A* **1983**, *A39*, 158.
(17) Cromer, D. T.; Waber, J. T. *International Tables for X-ray Crystallography*; Kynoch Press: Birmingham, England, 1974; Vol. IV, (a) Table 2.2b; (b) Table 2.3.1.
(18) Schrock, R. R.; Osborn, J. A. *J. Am. Chem. Soc.* **1976**, *98*, 2134.